ChemPubSoc Europe

DOI: 10.1002/ejoc.201600489

EurJOC European Journal of Organic Chemistry

Full Paper

FRET Rods

FRET Pairs with Fixed Relative Orientation of Chromophores

Pablo Wessig,*[a] Nicole Behrends,[a] Michael U. Kumke,*[a] and Ursula Eisold[a]

Dedicated to Professor Jochen Mattay on the occasion of his 70th birthday

Abstract: Synthetic routes to different oligospirothioketal (OSTK) Förster resonance energy transfer (FRET) constructs are described and the photophysics of these constructs were explored in different solvents. The FRET efficiencies were determined from the experimental data and compared with theoretical values. The influence of the outstanding rigidity of the novel OSTK compounds on the FRET is discussed.

Introduction

Mechanical forces represent a major factor in the modulation of cellular processes at different levels, such as adhesion to surfaces, the stiffness of cell membranes, or in the proliferation and differentiation of cells.[1] In general, two kinds of forces can be distinguished based on their origin: Exogenous and endogenous. Exogenous forces are caused, for example, by gravity or fluid shear, whereas endogenous forces originate from osmotic pressure or from proteins (e.g., motor proteins).[2] The measurement of the impact of such diverse forces on cells in vivo is a major challenge. Progress is strongly coupled to innovations in experimental methods (instruments but also suitable molecular probes).

The development/progress of force-based microscopic techniques, such as atomic force microscopy (AFM), and the availability of genetically encoded (intrinsic) fluorescence probes (GFP-based probes) have advanced in vivo detection at a single-cell/molecule level.[3] Based on the tremendous progress made in genetic engineering, the labeling of specific proteins inside the cell or in the membrane, which react to different external force stimuli initiating a downstream signaling cascade or act as an origin of force themselves (e.g., motor proteins), is now being developed.[2] The latter approach is based on the concept of Förster resonance energy transfer (FRET) and transduces the force-related alteration in the relative positions of fluorescent molecules into an optical signal [in the case of intrinsic probes two GFPs act as a donor (D)–acceptor (A) pair]. In addition, extrinsic sensors utilizing the FRET concept are also applied. Here, D and A are separated by a linker and one side of the FRET pair is attached to a surface (anchor side) and the other side to the cell surface (e.g., by specific binding through an antibody–antigen interaction)[3c] to monitor the forces between the cell surface and an extracellular matrix or between two cells. The force is also measured on the basis of the alteration of the FRET efficiency. The linker connecting the D–A pair is here a key element for the dynamic range of accessible forces.

Intrinsic as well as extrinsic FRET sensors are further defined by the specific spectroscopic parameters of the D–A pair, which defines the distance range (and therefore also the force range) accessible by a specific pair. Here, the so-called Förster radius R_0 is commonly used as a reference parameter. It describes the distance between D and A at which the efficiency of the FRET is 50 %. As a rule of thumb, a specific FRET pair can be used to monitor distance alterations in the range $0.5R_0 < r < 2R_0$. The combination of different intrinsic (spectroscopic) properties of D and A determine the value of R_0 [see Equation (1)]. The overlap integral J is defined by the spectral overlap between the donor emission and acceptor absorption spectra and is a measure of the overall number of resonant transitions for D and A. Achieving an improvement in J is a frequently used approach to increase R_0. Also, the fluorescence quantum yield of D has been addressed to pushinfluence R_0. On the other hand, the influence of the orientation factor κ^2 [see Equation (2)] has also been recognized but attempts to tailor this parameter are sparse. The parameter κ^2 relates the relative orientation of the transition dipole moments of D and A in space and is defined by the dot product of the respective unit vectors $\hat{d}$, $\hat{a}$, and $\hat{r}$ [see Equation (2a)] or, more handily, by the respective angles [see Equation (2b)].[4]

$$R_0 = \left(\frac{9000(\ln 10)\kappa^2\varphi_D J(\lambda)}{128\pi^5 N n^4}\right)^{\frac{1}{6}} \quad (1)$$

$$\kappa^2 = \left(\hat{d}\cdot\hat{a} - 3\cdot[\hat{d}\cdot\hat{r}]\cdot[\hat{a}\cdot\hat{r}]\right)^2 \quad (2a)$$

$$\kappa^2 = (cos\theta_T - 3cos\theta_D cos\theta_A)^2 \quad (2b)$$

$$E_{theor} = \frac{R_0^6}{R_0^6 + R^6} \quad (3)$$

The influence of κ^2 on the calculated donor (D) acceptor (A) distance can be large. For a D–A couple in solution, both free

[a] Institut für Chemie, Universität Potsdam,
Karl-Liebknecht-Str. 24–25, 14476 Potsdam, Germany
E-mail: wessig@uni-potsdam.de
http://ag-wessig.chem.uni-potsdam.de

Supporting information for this article is available on the WWW under http://dx.doi.org/10.1002/ejoc.201600489.

to rotate, κ^2 will be 2/3. In cases in which D and/or A are linked to a (macro)molecule, the rotational freedom can be distinctly altered. Depending on the nature of the linker and the chemical microenvironment created by the (macro)molecule, limitations in the accessible space due to intramolecular interactions or due to conformational hindrance can lead to distinct alterations in the value of κ^2. The miscalculation of κ^2 can cause an error of up to 40 % in the calculation of R_0.[4a] The situation may become even more complex in cases in which the κ^2 value and the D–A distance are no longer independent.[5]

Measurement of the forces should be possible if the two fluorescent dyes of a FRET pair are rigidly connected (and subsequently fully controlled) by a molecular rod (R). In view of the functional principles one can distinguish between two borderline cases, which are depicted in Figure 1. The first case exists if, in the "idle state", the transition moments (green arrows) of the donor and acceptor are collinear with respect to each other and to the line connecting D and A (Figure 1, a). Under these circumstances, the orientation factor κ^2 reaches the maximum possible value of 4. If the FRET rod is bent by an external stimulus (blue arrows) the FRET efficiency should decrease as a result of the decreasing κ^2 [cf. Equation (2)]. It should be noted that, at the same time, the distance between D and A is decreased, which should lead to an increase in the FRET efficiency. A simple estimate shows that the diminishing value of κ^2 dominates for a small amount of bending (see the Supporting Information). The second case occurs when the transition moments of D and A are arranged perpendicularly to each other and, additionally, the transition moment of the acceptor (or the donor) is also perpendicular to the line connecting D and A in the "idle state" (Figure 1, b). According to Equation (2b), κ^2 is zero and no FRET should take place. Upon bending, the orthogonality between the transition moments is cancelled resulting in increasing FRET.

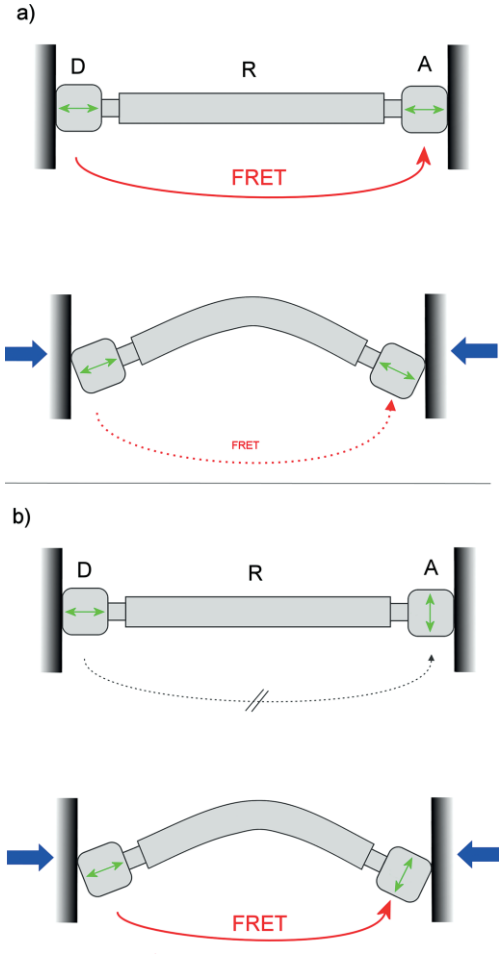

Figure 1. Functional principles of force-responsive FRET rods (D = donor, A = acceptor, R = molecular rod, green arrows = transition dipole moments, blue arrows = external stimuli).

To realize this concept, a FRET pair needs fluorescent dyes that can be rigidly connected with a molecular rod. Furthermore, the angle between the transition moments of the dyes and the direction axis of the rod should ideally be 0 or 90°. Rigidity is of the utmost importance because it has been shown that due to molecular vibrations very efficient FRET is observed even for orthogonally aligned transition dipole moments of D and A.[6] Based on our long-term experience with oligospiroketal (OSK) rods[7] and the recently developed oligospirothioketal (OSTK) rods,[8] we decided to use these rods in the current project. Very recently we reported on a new FRET pair consisting of a coumarin dye as donor and a dioxolobenzodioxole (DBD) dye[9] as acceptor.[10] The structures of these dyes meet the requirements stated above perfectly. Thus, in both cases the transition moments and the direction axes are nearly collinear and a point of connection to the OS(T)K rods is available (Figure 2). Herein we report on the synthetic routes to FRET pairs with rigid connection of the dyes in line with principle a in Figure 1.

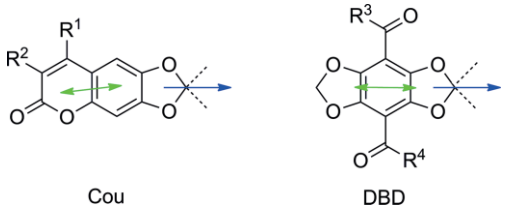

Figure 2. Coumarin (Cou) and [1,3]dioxolo[4,5-*f*][1,3]benzodioxole (DBD) dyes with transition moments (green) and direction axis of the rods (blue).

Results and Discussion

To compare the properties of the rigidly joined FRET pairs with more flexible counterparts we developed for each dye both a rigid and flexible combinable building block, hereinafter referred to as RC and FC dyes, respectively. The synthesis of the RC coumarin commenced with the commercially available 6,7-dihydroxycoumarin **1**. After silylation of the hydroxy groups, acetalization with 4-pivaloyloxycyclohexanone under Noyori conditions[11] gave the spirane **3**. After removal of the pivaloyl protecting group and oxidation we obtained the RC coumarin **5** (Scheme 1).

The FC coumarin building block was synthesized in two steps starting with the previously described carboxylic acid **6**.[1]

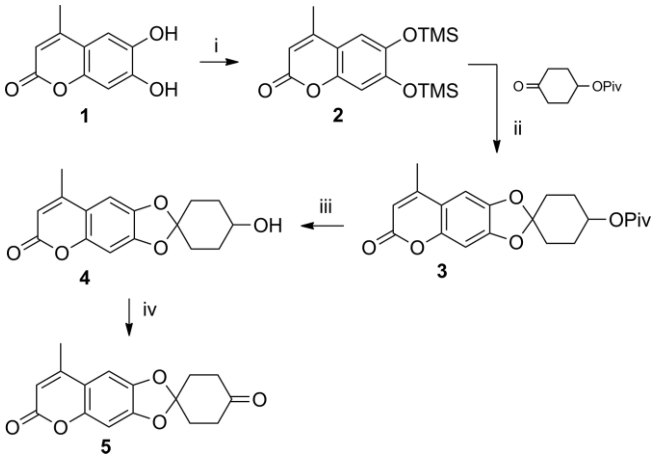

Scheme 1. Synthesis of ketone **5**. Reagents and conditions: i) TMSCl, Et_3N, toluene, quant.; ii) TMSOTf (cat.), DCM, 49 %; iii) $LiOH{\cdot}H_2O$, MeOH, 94 %; iv) Dess–Martin periodinane, DCM, 87 %.

Coupling with 4-hydroxypiperidine followed by oxidation of the hydroxy group afforded the FC coumarin **8** (Scheme 2).

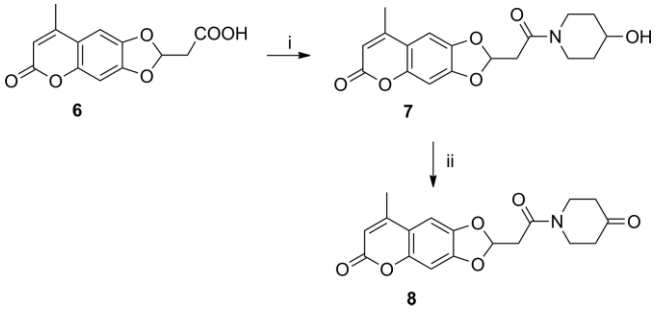

Scheme 2. Synthesis of ketone **8**. Reagents and conditions: i) 4-hydroxypiperidine, DCC, HOBt, DMF, 91 %; ii) Dess–Martin periodinane, DCM, 90 %.

The synthesis of the RC DBD building block proved to be considerably more sophisticated, because an acetalization in analogy to that used for coumarin **1** fails with DBD dyes. Therefore the spirane moiety has to be installed at an early stage of the synthesis. First, we prepared spirane **11** from the silyl-protected acetal of 4-hydroxycyclohexanone **9**[12] and hydroxyhydroquinone **10**. Oxidation with Fremy's salt {$K_2[ON(SO_3)_2]$} gave the quinone **12** in very good yield.[13] Reduction of **12** and subsequent protection of the resulting catechol with methoxymethyl (MOM) groups gave compound **13**. It should be noted that the MOM groups are necessary for complete twofold lithiation in the next step. After Li–Cu exchange, reaction with butyryl chloride afforded the MOM-catechol **14**. Deprotection with *p*-toluenesulfonic acid (pTSA) gave the nonfluorescent catechol **15** quantitatively. In the next step, the DBD skeleton was completed by 4-(dimethylamino)pyridine (DMAP)-catalyzed cyclization[14] with benzyl propiolate to give DBD dye **16**. The last step consists in the oxidation of the secondary hydroxy group to give the RC DBD building block **17** (Scheme 3).

The FC DBD building block **20** was prepared in a similar way to FC coumarin **8** starting from the previously described DBD acid **18** (Scheme 4).[9c]

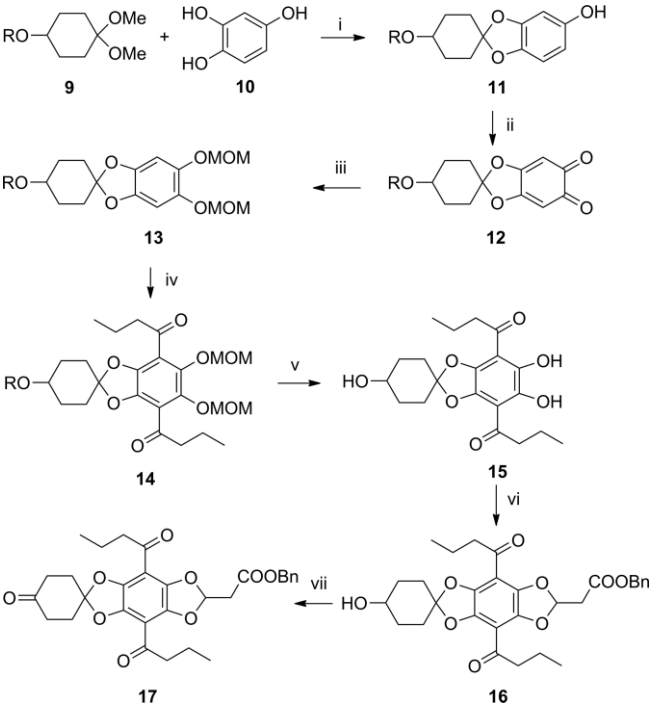

Scheme 3. Synthesis of ketone **17** (R = TBDMS). Reagents and conditions: i) PPTSA, toluene, 95 %; ii) $K_2[ON(SO_3)_2]$, KH_2PO_4 (pH 5–6), MeOH/acetone (1:3), 89 %; iii) 1. PtO_2, H_2, THF, 2 h; 2. NaH, MOMBr, –10 °C, 91 %; iv) 1. BuLi, CuI, THF; 2. butyryl chloride, 90 %; v) pTSA, MeOH, quant.; vi) benzyl propiolate, DMAP, DCM, 91 %; vii) Dess–Martin periodinane, DCM, 60 %.

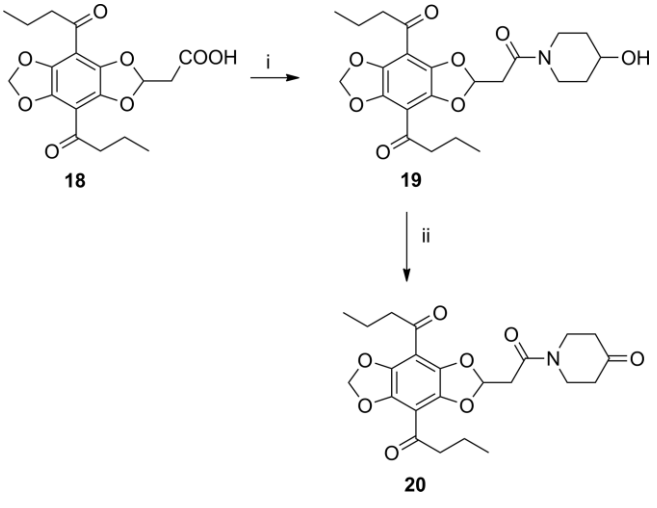

Scheme 4. Synthesis of ketone **20**. Reagents and conditions: i) 4-hydroxypiperidine, DCC, HOBt, DCM, quant.; ii) $(COCl)_2$, DMSO, DCM, 58 %.

With the RC (**5**, **17**) and FC (**8**, **20**) building blocks in hand we next investigated their combination with OSK rods. For this purpose we performed model reactions with diol **21**[15] by using the double-activation method (here cyclohexanone was the placeholder for the other dye).[7a] Unfortunately, the reaction between ketone **5** and diol **21** provided only the symmetric OSK rod **22** bearing two coumarin chromophores instead of the desired unsymmetrical rod (Scheme 5).

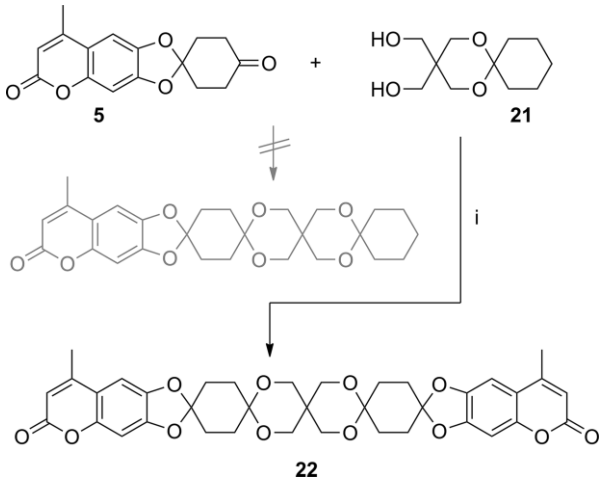

Scheme 5. Formation of rod **22**. Reagents and conditions: i) 1. NaH, TMSCl; 2. TMSOTf, 83 %.

The same result was obtained when the FC building block **8** was used instead of **5** (Scheme 6). This behavior, which is the consequence of several transacetalization steps, has frequently been observed in the past and is the principal disadvantage of OSK rods. The considerably lower solubility of symmetrical OSK rods is the main driving force for this outcome.

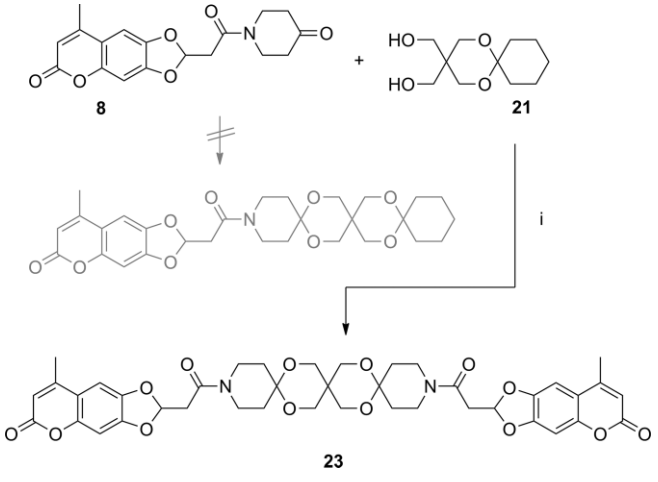

Scheme 6. Formation of compound **23**. Reagents and conditions: i) 1. NaH, TMSCl; 2. TMSOTf, 39 %.

Very recently we reported on oligospirothioketal (OSTK) rods, which differ from OSK rods in that one or more ketals are replaced by thioketals.[5] In contrast to ketals, the formation of thioketals from dithiols and ketones is not an equilibrium reaction and thioketals are significantly more stable towards hydrolytic conditions than ketals. For this reason we hypothesized that OSTK rods could circumvent the problems outlined in Scheme 5 and Scheme 6. To this end, we used diol **24**[8,16] bearing a 1,3-dithiane instead of a 1,3-dioxane and smoothly obtained coumarins **26** and **27** in satisfactory yields by using the double-activation method (Scheme 7).[7a] For the preparation of the analogous products with DBD dyes (**28** and **29**), it proved beneficial to apply Noyori conditions[11] with compound **25**, prepared from **24** by silylation in quantitative yield (Scheme 7).

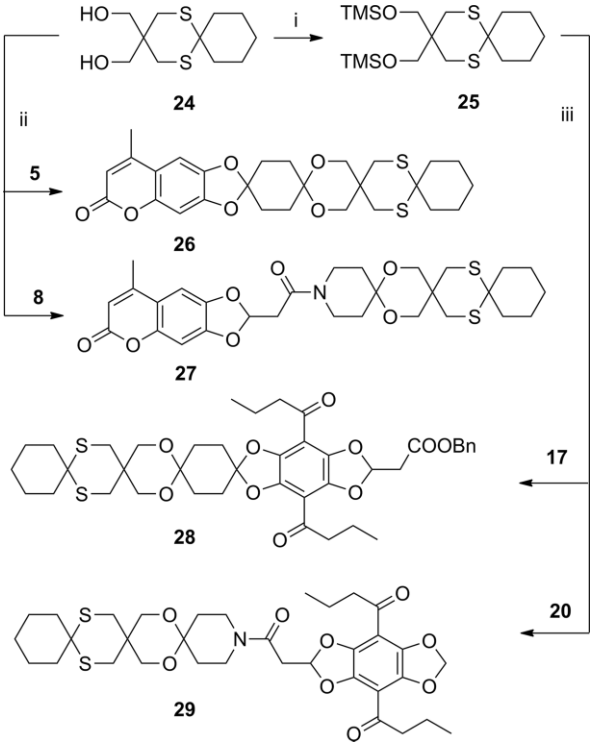

Scheme 7. Synthesis of compounds **26**–**29**. Reagents and conditions: i) TMSCl, Et_3N, toluene, quant.; ii) 1. NaH, TMSCl; 2. TMSOTf, Et_2O, 74 % (**26**), 55 % (**27**); iii) TMSOTf, DCM, 78 % (**28**), 93 % (**29**).

After these preliminary studies we turned our attention to the synthesis of Cou-DBD FRET pairs. Starting with the previously developed building block **30**,[8] the coumarin diol **31** was obtained by the iodine-catalyzed formation of the thioketal followed by removal of the TBDMS groups by HF. It should be noted that silyl groups are ideally suited for the protection of hydroxy groups in the presence of thiol groups due to the low S–Si affinity compared with the high O–Si affinity. Finally, **31** was converted into the bis-silyl ether **32**, which smoothly reacted with **17** to yield the rigid FRET rod **33** and with **20** to form the semi-flexible FRET rod **34** (Scheme 8 and Scheme 9).

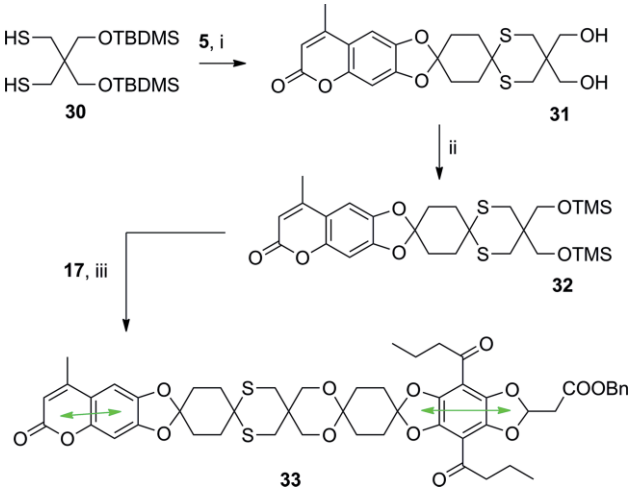

Scheme 8. Synthesis of FRET pair **33**. Reagents and conditions: i) 1. I_2; 2. HF, DCM, 87 %; ii) TMSCl, Et_3N, toluene, quant.; iii) TMSOTf, DCM, 64 %.

Table 1. Spectroscopic properties of single and double labeled rods **26**, **29**, **33**, and **34**.

	Solvent	Φ_D	Φ_A	ε_D (340 nm) [L/mol cm]	ε_A (450 nm) [L/mol cm]	τ_D [ns]	τ_{DA} [ns]	τ_A [ns]	E (Φ)	E (τ)
26	acetone	0.12 ± 0.006	–	9240 ± 460	–	0.8 ± 0.1	–	–	–	–
	$CHCl_3$	0.27 ± 0.01	–	12300 ± 620	–	1.7 ± 0.1	–	–	–	–
29	acetone	–	0.54 ± 0.03	–	1950 ± 100	–	–	22.5 ± 0.1	–	–
	$CHCl_3$	–	0.65 ± 0.03	–	2320 ± 120	–	–	24.1 ± 0.1	–	–
33	acetone	0.01 ± 0.001	0.58 ± 0.03	9330 ± 470	2840 ± 140	0.1 ± 0.03 (68 %) 1.2 ± 0.1 (32 %)	18.9 ± 0.1	18.9 ± 0.1	0.92 ± 0.01	0.88 ± 0.05
	$CHCl_3$	0.01 ± 0.001	0.71 ± 0.04	13600 ± 680	3200 ± 160	0.1 ± 0.03 (93 %) 1.8 ± 0.1 (7 %)	22.3 ± 0.1	22.3 ± 0.1	0.96 ± 0.01	0.95 ± 0.02
34	acetone	0.02 ± 0.001	0.60 ± 0.03	9700 ± 490	1455 ± 70	0.5 ± 0.1	18.1 ± 0.1	18.1 ± 0.1	0.83 ± 0.02	0.38 ± 0.2
	$CHCl_3$	0.05 ± 0.003	0.74 ± 0.04	13900 ± 700	1855 ± 90	1.2 ± 0.1	22.5 ± 0.1	22.5 ± 0.1	0.81 ± 0.02	0.30 ± 0.1

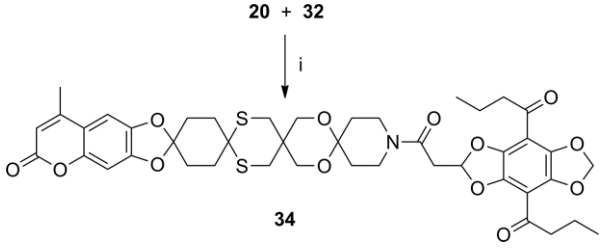

Scheme 9. Synthesis of FRET pair **34**. Reagents and conditions: i) TMSOTf, DCM, 50 %.

The mono- and double-labeled OSTK rods were characterized by absorption and fluorescence spectroscopy. With respect to the latter, steady-state as well as time-resolved data were acquired. In general, the dyes show a distinct solvent dependence of their photophysical properties independent of the attachment to an OSTK rod unit (see Table 1 and Figure 3).

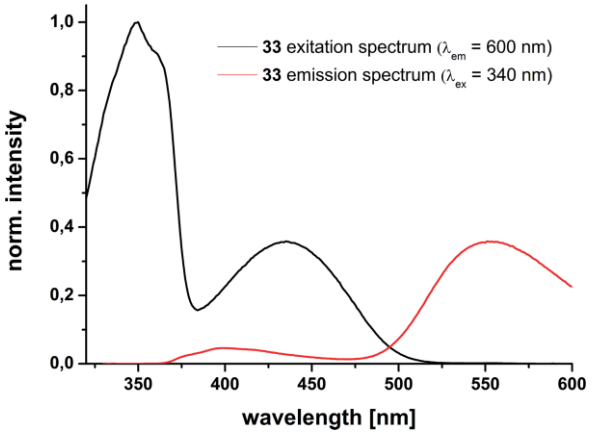

Figure 3. Excitation and emission spectra of **33** in $CHCl_3$.

Single-Labeled OSTK Rods 26 and 29

The spectroscopic properties of the coumarin do not change upon linking to the OSTK rod. No change in the spectral positions of the absorption or fluorescence emission compared with the coumarin parent compound (**6**) is found, because the "direct" substituents at the 6- and 7-positions are not altered. Upon excitation an intramolecular charge transfer ("push–pull" system) is initiated, which is, in general, the origin of the observed photophysics of the 6,7-dialkoxycoumarins. The expected solvent dependence can be observed as a slight bathochromic shift in the absorption and fluorescence bands of the Cou-OSTK rod upon changing the solvent polarity. More distinct are the alterations in the extinction coefficients and the fluorescence quantum yields Φ as well as in the fluorescence decay times τ. Changing the solvent from acetone to chloroform leads to an increase in these photophysical parameters. The fluorescence decay curves (λ_{ex} = 340 nm, λ_{em} = 420 nm) of the Cou-OSTK rod **26** show monoexponential behavior in polar and nonpolar solvents. The fluorescence decay time for the Cou-OSTK rod in acetone (τ = 0.8 ns) is shorter than that in chloroform (τ = 1.7 ns) and correlates with the results of the steady-state fluorescence measurements and quantum yields (Table 1).

The spectroscopic properties of the DBD dyes have previously been reported to be sensitive to the local environment and this is especially reflected in the huge alteration of the spectral intensity distribution.[9a] The Stokes shift ($\Delta\lambda$) of more than 100 nm for the DBD-OSTK rod **29** is very large. In acetone it is about 117 nm (λ_{abs} = 419 nm, λ_{em} = 536 nm) and in chloroform it is about 124 nm (λ_{abs} = 427 nm, λ_{em} = 551 nm). The solvent dependence of the spectroscopic properties is also evidenced by the fluorescence parameters Φ and τ. The fluorescence decay time (λ_{ex} = 450 nm, λ_{em} = 650 nm) for the DBD-OSTK rod **29** in acetone (τ = 22.5 ns) is slightly shorter than that in chloroform (τ = 24.1 ns). This is complementary to the results for the fluorescence quantum yields Φ, which were determined to be 0.54 and 0.65 in acetone and chloroform, respectively.

Double-Labeled OSTK Rods 33 and 34

The fluorescence emission of the Cou-OSTK rod (donor) shows a very good spectral overlap with the absorption of the DBD-OSTK rod (acceptor, see the Supporting Information). From the spectral overlap integral the theoretical Förster distance of **33** was calculated by Equation (1) with κ^2 = 3.9 to be R_0 = 4.8 nm. The distance R between the donor and acceptor is 1.9 nm. Based on these data, a very efficient FRET with $E \geq 99$ % was expected for compound **33** and confirmed by the experimental results (see below).

The fluorescence decay curve of the rigid FRET-OSTK rod **33** in chloroform shows a biexponential fluorescence decay. The strong quenching of the donor fluorescence yields a very short fluorescence decay time of τ_1 = 0.1 ns (93 %). The small contribution of the second decay time τ_2 = 1.8 ns (7 %) was attributed to a minor amount of unbound coumarin precursor still in

the sample. The experimental FRET efficiency for the rigid FRET-OSTK rod **33** was calculated by Equation (3) using the fluorescence decay times as well as the fluorescence quantum yields. Both sets of data are in excellent agreement and for both solvents FRET efficiencies of >90 % were determined, which fit well with the theoretical value calculated with Equation (3).

OSTK rod **34** was investigated as a reference compound in which the DBD dye is connected to a flexible linker yielding a distinctly higher degree of freedom with respect to the rotation of the DBD dye relative to the Cou dye. The overall maximum distance between donor and acceptor was approximately the same (ca. 2.2 nm), but because of the greater flexibility the κ^2 value was reduced to 2/3, which yielded a smaller R_0 value of 2.7 nm. Consequently a reduced FRET efficiency was expected. From Table 1 it can be seen that in the case of compound **34** the calculated FRET efficiencies based on the fluorescence quantum yields and the fluorescence decay times are distinctly different, and the solvent seems to have no influence on the determined values. This observed difference in *E* may be an indication of the formation of an equilibrium between two (limiting) forms of **34** ("limiting" conformers). One "limiting" conformer is represented by the DBD dye unit rotated in such a way that it becomes closer towards the rod and the coumarin unit. Here, the distance between the two dyes (D–A distance) is highly reduced, but at the same time the relative orientation of the transition dipole moments (κ^2 influence) could be less efficient for FRET.

In the second "limiting" conformer an elongated form is present in which the distance is longer but due to an almost collinear orientation of the transition dipole moments (κ^2 becomes close to four) a more efficient FRET may be operative. Although for very efficient energy transfer the corresponding fluorescence decay time becomes extremely short and is consequently not resolvable, in the case of less efficient energy transfer a quenched fluorescence decay time can be measured. For such a system only in the quantum yield measurements will both (limiting) conformers contribute to the calculation of the FRET efficiency, whereas in the case of decay time measurements the "dark form" does not contribute and a smaller FRET efficiency is determined. The spectroscopic properties of **34**, compared with **33**, underline the strong influence of κ^2 on the FRET efficiency. It should be noted that in **33** as well as in **34** the distance between D and A is small (<5 nm) and the dipole approximation of the FRET theory may not be fully applicable.[16] The relative orientation of D and A is highly fixed, especially in **33**, and an averaging out of errors should not be operative, which makes the good agreement between the theoretical and experimental FRET efficiency for **33** especially interesting from a fundamental point of view. Work is in progress to investigate this topic in greater detail by systematically altering the distance between D and A by using the unique rigidity of the OSTK rods.

Conclusions

The FRET system based on OS(T)K rods has been successfully developed and compared with other rigid spacer concepts the rods show some distinct features that make them highly attractive as building blocks for further development in the field of optical force detection. The relative orientation of D and A is highly fixed especially in **33** and an averaging out of errors should not be operative, which also makes the good agreement between theoretical and experimental FRET efficiencies interesting from a fundamental point of view. Compared with recently reported FRET systems with orthogonally fixed alignment of D and A, no distinct influence of vibrations or "environmental noise" was observed.[6,18] The excellent agreement between theoretically expected and experimentally found FRET efficiencies underlines the outstanding rigidity of the OS(T)K rods. The minimization of vibrational influences on FRET efficiency is a prerequisite for application in force measurements based on alterations in the fluorescence parameters of a D–A pair because it will significantly improve the precision of the measurement by limiting uncertainties due to force-unrelated motions.[17]

With the successful proof-of-concept the next steps will include a systematic increase in the OS(T)K rod length to monitor the contour length of the rods to determine the critical length at which significant alterations, for example, due to vibrational motions, become effective. Moreover, complementary constructs carrying D and A with an orthogonal orientation of their respective transition dipole moments as well as OS(T)K rods with a link adding flexibility (again) are currently being synthesized to create a tool box of linkers. We are also exploring the incorporation of OS(T)K rods into vesicles as biomimetic systems for cells, which will be combined with AFM, serving as an artificial force stimulus, to further develop the concept of optical force measurements based on our novel probes.

Experimental Section

General Information: See the Supporting Information.

4-Methyl-6,7-bis[(trimethylsilyl)oxy]-2*H*-chromen-2-one (2): Anhydrous NEt_3 (9.48 mg, 93.67 mmol, 6.0 equiv.) and TMSCl (10.18 g, 93.67 mmol, 6.0 equiv.) were added to a suspension of 6,7-dihydroxy-4-methylcoumarin (**1**; 3.00 g, 15.61 mmol) in anhydrous toluene (100 mL). The reaction mixture was stirred overnight at room temperature, filtered through Celite®, washed with petroleum ether (PE), and the solvent was evaporated. The residue was suspended in PE and filtered through Celite® once more. Evaporation of the solvent yielded **2** (15.20 g, 15.45 mmol, 99 %) as a white solid, m.p. 57–60 °C. ^{1}H NMR (300 MHz, $CDCl_3$): δ = 6.99 (s, 1 H), 6.82 (s, 1 H), 6.15 (s, 1 H), 2.35 (s, 3 H), 0.31 (s, 9 H), 0.27 (s, 9 H) ppm. ^{13}C NMR (75 MHz, $CDCl_3$): δ = 161.4, 152.0, 150.5, 149.2, 143.7, 115.1, 114.0, 112.5, 108.5, 18.6, 0.2 ppm. IR (ATR): $\tilde{\nu}$ = 3155, 2960, 2787, 2769, 1722, 1666, 1609, 1552, 1503, 1418, 1387, 1368, 1292, 1249, 1227, 1214, 1170, 1151, 1061, 1033, 1005, 941, 904, 884, 865, 843, 758, 695, 670, 605 cm^{-1}. HRMS: calcd. for $C_{16}H_{25}O_4Si_2$ 337.1291 $[M + H]^+$; found 337.1263.

8′-Methyl-6′-oxo-6′*H*-spiro[cyclohexane-1,2′-[1,3]dioxolo[4,5-*g*]chromen]-4-yl Pivalate (3): A solution of **2** (4.00 g, 11.98 mmol) and 4-oxocyclohexyl pivalate (2.47 g, 12.48 mmol, 1.05 equiv.) in anhydrous DCM (150 mL) was treated with 2 drops of TMSOTf. After stirring overnight the solvent was removed under reduced pressure and the residue was purified by flash silica gel column chromatography [Hex/ethyl acetate (EE), 5:1] to yield **3** (2.15 g, 5.77 mmol,

49 %) as a white solid, m.p. 215–218 °C. ^{1}H NMR (300 MHz, $CDCl_3$): δ = 6.89 (s, 1 H), 6.76 (s, 1 H), 6.14 (d, ^4J = 0.9 Hz, 1 H), 5.04–4.95 (m, 1 H), 2.38–2.32 (m, 3 H), 2.19–1.90 (m, 8 H), 1.26–1.17 (m, 9 H) ppm. ^{13}C NMR (75 MHz, $CDCl_3$): δ = 177.7, 161.3, 152.4, 150.6, 150.4, 144.6, 119.7, 113.5, 111.9, 101.9, 98.3, 67.9, 38.9, 31.0, 27.2, 27.1, 19.1 ppm. IR (ATR): $\tilde{\nu}$ = 3056, 2968, 2940, 2872, 1719, 1623, 1583, 1493, 1452, 1399, 1376, 1344, 1266, 1249, 1228, 1206, 1165, 1150, 1138, 1118, 1065, 1043, 1000, 972, 921, 896, 846, 808, 769, 741 cm^{-1}. HRMS: calcd. for $C_{21}H_{24}O_6$ 372.1573 [M]$^+$; found 372.1565.

4-Hydroxy-8′-methyl-6′*H*-spiro[cyclohexane-1,2′-[1,3]dioxolo-[4,5-*g*]chromen]-6′-one (4): A solution of **3** (100 mg, 0.27 mmol) and LiOH·H_2O (33 mg, 0.81 mmol, 3.0 equiv.) in MeOH (10 mL) was stirred at room temperature until complete conversion of **3**, monitored by TLC. The organic layer was washed with 1 N HCl and brine and extracted with DCM (3×). The combined organic layers were dried with $MgSO_4$ and concentrated under reduced pressure. The resulting residue was purified by flash silica gel column chromatography (DCM/MeOH, 100:1) to yield **4** (73 mg, 0.25 mmol, 94 %) as a white solid, m.p. 145 °C. ^{1}H NMR (300 MHz, $CDCl_3$): δ = 6.92–6.87 (m, 1 H), 6.81–6.71 (m, 1 H), 6.14 (d, ^4J = 0.9 Hz, 1 H), 4.05–3.94 (m, 1 H), 2.39–2.33 (m, 3 H), 2.26–2.14 (m, 2 H), 2.05–1.78 (m, 6 H) ppm. ^{13}C NMR (75 MHz, $CDCl_3$): δ = 161.5, 152.6, 150.9, 150.4, 144.8, 120.1, 113.4, 111.8, 101.9, 98.2, 66.4, 31.2, 30.7, 19.1 ppm. IR (ATR): $\tilde{\nu}$ = 3879, 3078, 2771, 2596, 2535, 2297, 2233, 1707, 1624, 1581, 1494, 1453, 1401, 1368, 1346, 1270, 1249, 1207, 1142, 1119, 1071, 1045, 979, 951, 924, 896, 854, 809, 770, 743 cm^{-1}. HRMS: calcd. for $C_{16}H_{16}O_5$ 288.0998 [M]$^+$; found 288.0990.

8′-Methyl-6′*H*-spiro[cyclohexane-1,2′-[1,3]dioxolo[4,5-*g*]chromene]-4,6′-dione (5): Dess–Martin periodinane (DMP; 668 mg, 1.58 mmol, 1.1 equiv.) was added to a solution of **4** (413 mg, 1.43 mmol) in anhydrous DCM (50 mL). The mixture was stirred at room temperature overnight and then washed with an aqueous solution of $NaHCO_3$/$Na_2S_2O_3$ (250 g/L, 3×) and brine, and extracted several times with DCM. The combined organic layers were dried with $MgSO_4$, evaporated, and the resulting residue was purified by flash silica gel column chromatography (PE/EE, 3:1) to yield **5** (358 mg, 1.25 mmol, 87 %) as a white solid, m.p. >180 °C (decomp.). ^{1}H NMR (300 MHz, $CDCl_3$): δ = 6.97 (s, 1 H), 6.83 (s, 1 H), 6.18–6.15 (m, 1 H), 2.73–2.60 (m, 5 H), 2.44–2.33 (m, 8 H) ppm. ^{13}C NMR (75 MHz, $CDCl_3$): δ = 207.3, 161.1, 152.3, 150.5, 150.2, 144.3, 118.1, 113.8, 112.2, 102.4, 98.5, 36.9, 33.8, 19.0 ppm. IR (ATR): $\tilde{\nu}$ = 3436, 3120, 3043, 2934, 2903, 1781, 1708, 1621, 1579, 1493, 1450, 1417, 1400, 1364, 1348, 1326, 1273, 1238, 1149, 1115, 1059, 1043, 1008, 959, 930, 809, 776, 761, 745, 707 cm^{-1}. HRMS: calcd. for $C_{16}H_{14}O_5$ 286.0841 [M]$^+$; found 286.0842.

2-[2-(4-Hydroxypiperidin-1-yl)-2-oxoethyl]-8-methyl-6*H*-[1,3]dioxolo[4,5-*g*]chromen-6-one (7): 4-Hydroxypiperidine (20 mg, 0.20 mmol, 1.05 equiv.), *N,N′*-dicyclohexylcarbodiimide (DCC; 28 mg, 0.21 mmol, 1.1 equiv.), and 1-hydroxybenzotriazole (HOBt; 43 mg, 0.21 mmol, 1.1 equiv.) were added to a solution of **6** (50 mg, 0.91 mmol) in anhydrous DMF (10 mL). After stirring overnight at room temperature the precipitate was filtered through Celite®. The organic layer was washed with 0.1 N HCl, aq. $NaHCO_3$, and brine and dried with $MgSO_4$. The solvent was evaporated and the residue purified by flash silica gel column chromatography (DCM/MeOH, 100:1) to yield **7** (60 mg, 0.17 mmol, 91 %) as a white solid, m.p. 98–100 °C. ^{1}H NMR (300 MHz, $CDCl_3$): δ = 6.91 (s, 1 H), 6.76 (s, 1 H), 6.71 (t, ^3J = 5.09 Hz, 1 H), 6.12 (s, 1 H), 3.90–4.09 (m, 2 H), 3.62–3.75 (m, 1 H), 3.17–3.38 (m, 2 H), 3.04 (d, ^3J = 5.09 Hz, 2 H), 2.23 (m, 3 H), 1.87 (m, 2 H), 1.56 (m, 2 H) ppm. ^{13}C NMR (75 MHz, $CDCl_3$): δ = 165.4, 161.2, 152.5, 150.6, 150.4, 144.6, 113.8, 112.0, 111.0, 102.1, 98.2, 66.4, 42.8, 38.8, 38.4, 34.2, 33.5, 19.0 ppm. IR (ATR): $\tilde{\nu}$ = 3830, 3422, 3057, 2927, 2861, 2694, 2669, 1582, 1493, 1449, 1402, 1386, 1347, 1264, 1204, 1141, 1116, 1075, 1047, 1029, 1010, 961, 920, 856, 806, 779, 745, 711, 676, 640 cm^{-1}. HRMS: calcd. for $C_{18}H_{19}NO_6$ 345.1244 [M]$^+$; found 345.1221.

1-[2-(8-Methyl-6-oxo-6*H*-[1,3]dioxolo[4,5-*g*]chromen-2-yl)acetyl]piperidin-4-one (8): DMP (848 mg, 2.00 mmol, 1.1 equiv.) was added to a solution of **7** (628 mg, 1.82 mmol) in anhydrous DCM (80 mL). The mixture was stirred at room temperature overnight and then washed with an aqueous solution of $NaHCO_3$/$Na_2S_2O_3$ (250 g/L, 3×) and brine, and extracted several times with DCM. The combined organic layers were dried with $MgSO_4$, evaporated, and the resulting residue was purified by flash silica gel column chromatography (DCM/MeOH, 100:1) to yield **8** (561 mg, 1.63 mmol, 90 %) as a white solid, m.p. 174 °C. ^{1}H NMR (300 MHz, $CDCl_3$): δ = 6.92 (s, 1 H), 6.76 (s, 1 H), 6.74 (t, ^3J = 4.99 Hz, 2 H), 6.11 (s, 1 H), 3.93 (t, ^3J = 5.93 Hz, 2 H), 3.77 (t, ^3J = 6.12 Hz, 2 H), 3.14 (d, ^3J = 4.90 Hz, 2 H), 2.51 (q, ^3J = 5.65 Hz, 4 H), 2.33 (s, 3 H) ppm. ^{13}C NMR (75 MHz, $CDCl_3$): δ = 205.8, 166.0, 161.0, 152.2, 150.5, 150.4, 144.5, 113.9, 112.3, 110.7, 102.2, 98.4, 44.1, 40.9, 40.7, 40.5, 38.5, 19.0 ppm. IR (ATR): $\tilde{\nu}$ = 3126, 2933, 2858, 1730, 1644, 1583, 1493, 1446, 1402, 1381, 1366, 1346, 1263, 1221, 1201, 1165, 1142, 1092, 1037, 963, 918, 888, 847, 824, 806, 778, 745, 728, 709, 648 cm^{-1}. HRMS: calcd. for $C_{18}H_{17}NO_6$ 343.1056 [M]$^+$; found 343.1064.

***tert*-Butyl[(4,4-dimethoxycyclohexyl)oxy]dimethylsilane (9):** A solution of *tert*-butyl[(4,4-dimethoxycyclohexyl)oxy]dimethylsilane (1.5 g, 6.57 mmol) and *p*TSA (12.5 mg, 0.07 mmol, 0.01 equiv.) in trimethyl orthoformate/MeOH (5:1, 24 mL) was stirred until complete conversion (1 h), controlled by TLC. NEt_3 (100 μL) was added and the solvent was removed in vacuo. The residue was purified by flash silica gel column chromatography (Hex/EE, 20:1) to yield **9** (1.8 g, 6.56 mmol, quant.) as a colorless oil. ^{1}H NMR (300 MHz, $CDCl_3$): δ = 3.81–3.65 (m, 1 H), 3.11–3.00 (m, 6 H), 2.04–1.83 (m, 2 H), 1.71–1.46 (m, 6 H), 1.05–0.92 (m, 9 H), 0.11 to –0.01 (m, 6 H) ppm. ^{13}C NMR (75 MHz, $CDCl_3$): δ = 100.0, 69.3, 47.9, 47.5, 32.0, 29.4, 26.4, –4.2 ppm. IR (ATR): $\tilde{\nu}$ = 2951, 2930, 2856, 1472, 1462, 1435, 1375, 1249, 1236, 1132, 1102, 1051, 1019, 935 914, 905, 865, 850, 833, 809, 771, 675 cm^{-1}.

4′-[(*tert*-Butyldimethylsilyl)oxy]spiro[benzo[*d*][1,3]dioxole-2,1′-cyclohexan]-5-ol (11): Anhydrous toluene (150 mL) and pyridinium *p*-toluenesulfonate (PPTSA; 17.0 mg, 0.07 mmol, 0.01 equiv.) were added to a two-necked flask equipped with a distillation apparatus and the mixture was stirred and heated to 80 °C. Benzene-1,2,4-triol (**10**; 835.4 mg, 6.62 mmol) was added and the mixture was heated at reflux. Compound **9** (2.0 g, 7.26 mmol, 1.10 equiv.) was added in three portions every 15 min. The solution was then heated at reflux for an additional hour. After cooling the solvent was evaporated and the residue purified by flash silica gel column chromatography (PE/EE, 10:1) to yield **11** (2.1 mg, 6.30 mmol, 95 %) as a beige solid, m.p. 80–82 °C. ^{1}H NMR (300 MHz, $CDCl_3$): δ = 6.60–6.54 (m, 1 H), 6.39–6.33 (m, 1 H), 6.21 (dd, ^3J = 2.4, 8.3 Hz, 1 H), 3.99–3.91 (m, 1 H), 2.24–2.11 (m, 2 H), 1.94–1.70 (m, 7 H), 0.92 (s, 10 H), 0.09 (s, 7 H) ppm. ^{13}C NMR (75 MHz, $CDCl_3$): δ = 150.2, 148.1, 141.5, 118.6, 107.8, 105.8, 98.1, 66.4, 31.1, 30.5, 25.8, 18.1, –4.8 ppm. IR (ATR): $\tilde{\nu}$ = 3319, 3262, 3088, 2953, 2931, 2855, 2709, 1636, 1618, 1478, 1437, 1374, 1322, 1249, 1198, 1144, 1112, 1062, 1043, 1014, 964, 947, 896, 853, 830, 776, 712, 677, 641, 608 cm^{-1}. HRMS: calcd. for $C_{18}H_{28}O_4Si$ 336.1757 [M]$^+$; found 336.1763.

4′-[(*tert*-Butyldimethylsilyl)oxy]spiro[benzo[*d*][1,3]dioxole-2,1′-cyclohexane]-5,6-dione (12): Fremy's salt ($K_2NO_7S_2$, 12.54 g, 37.40 mmol, 2.50 equiv.) was added to a solution of KH_2PO_4 (1.4 g, 10.29 mmol, 0.55 equiv.) in H_2O (90 mL) at 0 °C. Compound **11** (6.29 g, 18.70 mmol, 1.0 equiv.) dissolved in MeOH/acetone (1:3,

20 mL) was added to the solution within 15 min. After stirring at 0 °C for 4 h, the suspension was stirred overnight at room temperature. The resulting yellow precipitate was washed with H_2O and extracted with DCM several times. The combined organic layers were dried with $MgSO_4$ and evaporated to yield **12** (2.1 mg, 6.30 mmol, 95 %) as an orange solid, m.p. 197–199 °C. ^{1}H NMR (300 MHz, $CDCl_3$): δ = 5.94 (m, 2 H), 4.10–3.99 (m, 1 H), 2.44–2.27 (m, 2 H), 1.90–1.76 (m, 6 H), 0.91 (s, 9 H), 0.17–0.01 (m, 6 H) ppm. ^{13}C NMR (75 MHz, $CDCl_3$): δ = 177.9, 161.0, 125.0, 101.1, 101.0, 64.7, 30.8, 30.6, 25.7, 18.0, –4.9 ppm. IR (ATR): $\tilde{\nu}$ = 3088, 3070, 2953, 2929, 2883, 2856, 1722, 1654, 1469, 1438, 1399, 1360, 1334, 1292, 1233, 1200, 1155, 1134, 1119, 1064, 1047, 1018, 962, 898, 866, 844, 816, 772, 631, 619 cm^{-1}. HRMS: calcd. for $C_{18}H_{26}O_5Si$ 350.1550 $[M]^+$; found 350.1569.

({5,6-Bis(methoxymethoxy)spiro[benzo[*d*][1,3]dioxole-2,1′-cyclohexan]-4′-yl}oxy)(*tert*-butyl)dimethylsilane (13): A suspension of **12** (1.16 g, 3.32 mmol) and PtO_2 (2 mg, 9.13 µmol, 0.001 equiv.) in dry THF (150 mL) was stirred under hydrogen [$p(H_2)$ = 1 atm] at room temperature. After the complete conversion of **12**, monitored by TLC (2 h), the solution was cooled to –10 °C under N_2. NaH (451.36 mg, 11.29 mmol, 3.4 equiv.) was added and the reaction mixture was stirred for 30 min. MOMBr (903 µL, 9.96 mmol, 3.0 equiv.) dissolved in dry THF (10 mL) was added dropwise within 15 min. The solution was stirred overnight at room temperature. The resulting white suspension was washed with H_2O and brine and extracted several times with Et_2O. The solvent was dried with $MgSO_4$, evaporated, and the residue was purified by flash silica gel column chromatography (PE/EE, 10:1) to yield **13** (1.34 g, 3.03 mmol, 91 %) as a colorless oil. ^{1}H NMR (300 MHz, $CDCl_3$): δ = 6.68 (s, 2 H), 5.10 (s, 4 H), 3.99–3.88 (m, 1 H), 3.53 (s, 6 H), 2.27–2.10 (m, 2 H), 1.95–1.69 (m, 6 H), 0.95–0.88 (m, 9 H), 0.08 (s, 6 H) ppm. ^{13}C NMR (75 MHz, $CDCl_3$): δ = 142.4, 142.4, 141.4, 141.3, 118.8, 100.8, 100.7, 96.9, 66.4, 56.1, 31.1, 30.5, 25.8, 18.1, –4.8 ppm. IR (ATR): $\tilde{\nu}$ = 2951, 2930, 2894, 2855, 1491, 1377, 1251, 1208, 1148, 1071, 1043, 962, 922, 874, 835, 772, 684, 623, 477 cm^{-1}. HRMS: calcd. for $C_{22}H_{36}O_7Si$ 440.2230 $[M]^+$; found 440.2209.

1,1′-{4′-[(*tert*-Butyldimethylsilyl)oxy]-5,6-bis(methoxymethoxy)spiro[benzo[*d*][1,3]dioxole-2,1′-cyclohexane]-4,7-diyl}bis(butan-1-one) (14): A solution of **13** (1.52 g, 3.45 mmol) in anhydrous THF (100 mL) was cooled to –60 °C. *n*BuLi (1.6 M, 5.61 mL, 8.98 mmol, 2.6 equiv.) was added over 10 min and the mixture stirred for 1.5 h at 0 °C. Anhydrous CuI (1.64 g, 8.64 mmol, 2.5 equiv.) was then added and the suspension stirred for 1.5 h. Then butyryl chloride (1.43 mL, 13.82 mmol, 4.0 equiv.) was added and the reaction mixture stirred for a further 2 h. An aqueous solution of NH_4Cl was added and the mixture extracted with Et_2O. The organic layer was dried with $MgSO_4$, evaporated, and the residue purified by flash silica gel column chromatography (PE/EE, 30:1) to yield **14** (1.80 g, 3.10 mmol, 90 %) as a pale-yellow oil. ^{1}H NMR (300 MHz, $CDCl_3$): δ = 5.01 (s, 4 H), 3.95 (br. s, 1 H), 3.47 (s, 6 H), 2.93–2.77 (m, 4 H), 2.27–2.09 (m, 2 H), 1.99–1.47 (m, 10 H), 1.03–0.93 (m, 6 H), 0.91 (s, 9 H), 0.07 (s, 6 H) ppm. ^{13}C NMR (75 MHz, $CDCl_3$): δ = 162.3, 140.9, 121.2, 100.5, 100.5, 66.0, 57.7, 57.7, 46.2, 46.2, 31.0, 30.5, 25.8, 18.1, 17.2, 17.2, 13.8, 13.7, 13.6, –4.9 ppm. IR (ATR): $\tilde{\nu}$ = 3095, 2959, 2934, 2879, 2858, 1738, 1708, 1462, 1433, 1377, 1359, 1280, 1252, 1242, 1213, 1158, 1138, 1112, 1094, 1079, 1054, 1003, 939, 859, 837, 813, 774, 676 cm^{-1}. HRMS: calcd. for $C_{30}H_{48}O_9Si$ 580.3068 $[M]^+$; found 580.3088.

1,1′-(4′,5,6-Trihydroxyspiro[benzo[*d*][1,3]dioxole-2,1′-cyclohexane]-4,7-diyl)bis(butan-1-one) (15): A solution of **14** (300 mg, 516 µmol) and *p*TSA·H_2O (1.28 mg, 6 µmol, 0.01 equiv.) in MeOH (7 mL) was stirred overnight. The solvent was evaporated and the residue washed with H_2O/DCM. The solvent was dried with $MgSO_4$ and evaporated to yield **15** (190 mg, 502 µmol, quant.) as a red solid, m.p. 190–192 °C. ^{1}H NMR (300 MHz, $CDCl_3$): δ = 4.14–3.93 (m, 1 H), 3.10–2.85 (m, 4 H), 2.34–2.18 (m, 2 H), 2.06–1.79 (m, 6 H), 1.79–1.64 (m, 4 H), 1.12–0.92 (m, 6 H) ppm. ^{13}C NMR (75 MHz, $CDCl_3$): δ = 205.2, 143.6, 143.6, 138.4, 119.6, 109.7, 109.6, 66.3, 45.5, 45.5, 30.9, 17.4, 17.4, 13.8 ppm. IR (ATR): $\tilde{\nu}$ = 3249, 3041, 2963, 2938, 2874, 1631, 1450, 1377, 1339, 1288, 1272, 1233, 1177, 1147, 1117, 1065, 1056, 1034, 1006, 979, 953, 938, 909, 878, 759 cm^{-1}. HRMS: calcd. for $C_{20}H_{26}O_7$ 378.1679 $[M]^+$; found 378.1686.

Benzyl 2-{4,8-Dibutyryl-4′-hydroxyspiro[benzo(1,2-*d*:4,5-*d*′)-bis([1,3]dioxole)-2,1′-cyclohexan]-6-yl}acetate (16): DMAP (125 mg, 1.02 mmol, 1.5 equiv.) was added to a solution of **15** (336 mg, 681 µmol) and benzyl prop-2-ynoate (120 mg, 750 µmol, 1.1 equiv.) in anhydrous DCM (8 mL) under N_2 at room temperature. After stirring overnight, the solvent was removed under reduced pressure. Purification of the residue by flash silica gel column chromatography (DCM/MeOH, 100:1) afforded **16** (406 mg, 621 µmol, 91 %) as an orange, vitreous solid. ^{1}H NMR (300 MHz, $CDCl_3$): δ = 7.36 (s, 5 H), 6.66 (t, ^3J = 5.0 Hz, 1 H), 5.20 (s, 2 H), 4.04–3.93 (m, 1 H), 3.11 (d, ^3J = 5.1 Hz, 2 H), 2.91–2.78 (m, 4 H), 2.30–2.14 (m, 2 H), 2.04–1.89 (m, 4 H), 1.88–1.80 (m, 2 H), 1.75–1.65 (m, 4 H), 1.04–0.92 (m, 6 H) ppm. ^{13}C NMR (75 MHz, $CDCl_3$): δ = 196.3, 167.5, 135.1, 128.6, 128.4, 128.2, 120.4, 109.5, 66.9, 66.5, 45.6, 40.0, 31.1, 30.9, 17.2, 13.8 ppm. IR (ATR): $\tilde{\nu}$ = 3525, 2960, 2938, 2874, 1737, 1684, 1439, 1370, 1282, 1174, 1101, 1051, 993, 750, 698, 603 cm^{-1}. HRMS: calcd. for $C_{30}H_{34}O_9$ 538.2203 $[M]^+$; found 538.2211.

Benzyl 2-{4,8-Dibutyryl-4′-oxospiro[benzo(1,2-*d*:4,5-*d*′)-bis([1,3]dioxole)-2,1′-cyclohexan]-6-yl}acetate (17): DMP (175 mg, 0.41 mmol, 1.5 equiv.) was added to a solution of **16** (148 mg, 0.27 mmol) in anhydrous DCM (10 mL) and the mixture was stirred overnight at room temperature. It was then washed with an aqueous solution of $NaHCO_3$/$Na_2S_2O_3$ (250 g/L, 2×) and brine. The organic layers were dried with $MgSO_4$, evaporated, and the resulting residue purified by flash silica gel column chromatography (DCM/MeOH, 100:1) to yield **17** (89 mg, 0.17 mmol, 60 %) as an orange, vitreous solid. ^{1}H NMR (300 MHz, $CDCl_3$): δ = 7.36 (s, 5 H), 6.69 (t, ^3J = 5.0 Hz, 1 H), 5.20 (s, 2 H), 3.13 (d, ^3J = 5.1 Hz, 2 H), 2.85 (t, ^3J = 7.2 Hz, 4 H), 2.70–2.57 (m, 4 H), 2.48–2.34 (m, 4 H), 1.78–1.61 (m, 4 H), 0.96 (t, ^3J = 7.4 Hz, 6 H) ppm. ^{13}C NMR (75 MHz, $CDCl_3$): δ = 207.5, 196.1, 167.4, 140.5, 140.3, 135.1, 128.6, 128.5, 128.3, 118.5, 110.2, 109.7, 67.0, 45.6, 40.0, 37.1, 33.7, 17.1, 13.8 ppm. IR (ATR): $\tilde{\nu}$ = 3033, 2963, 2936, 2875, 1739, 1722, 1687, 1472, 1455, 1439, 1416, 1401, 1369, 1285, 1217, 1177, 1118, 1104, 1065, 1046, 989, 889, 752, 699 cm^{-1}. HRMS: calcd. for $C_{30}H_{32}O_9$ 536.2046 $[M]^+$; found 536.2066.

1,1′-{2-[2-(4-Hydroxypiperidin-1-yl)-2-oxoethyl]benzo-(1,2-*d*:4,5-*d*′)bis([1,3]dioxole)-4,8-diyl}bis(butan-1-one) (19): 4-Hydroxypiperidine (46 mg, 0.45 mmol, 1.1 equiv.), DCC (102 mg, 0.49 mmol, 1.2 equiv.), and HOBt (67 mg, 0.49 mmol, 1.2 equiv.) were added to a solution of **18** (150 mg, 0.41 mmol) in anhydrous DCM (40 mL). After stirring overnight at room temperature the organic layer was washed with 0.1 N HCl, aq. $NaHCO_3$, and brine and dried with $MgSO_4$. The solvent was evaporated and the residue was purified by flash silica gel column chromatography (DCM/MeOH, 100:1) to yield **19** (182 mg, 0.41 mmol, quant.) as an orange solid, m.p. 90–91 °C. ^{1}H NMR (300 MHz, $CDCl_3$): δ = 6.71 (t, ^3J = 5.0 Hz, 1 H), 6.08 (s, 2 H), 4.14–3.82 (m, 2 H), 3.82–3.61 (m, 1 H), 3.37–3.17 (m, 2 H), 3.10 (d, ^3J = 4.9 Hz, 2 H), 3.03–2.70 (m, 4 H), 1.97–1.81 (m, 2 H), 1.77–1.61 (m, 4 H), 1.61–1.44 (m, 2 H), 0.95 (t, ^3J = 7.4 Hz, 6 H) ppm. ^{13}C NMR (75 MHz, $CDCl_3$): δ = 196.4, 165.3, 140.9, 140.7, 111.4, 110.0, 102.5, 66.7, 45.6, 43.1, 39.1, 38.3, 34.3, 33.7, 17.1, 13.7 ppm. IR (ATR): $\tilde{\nu}$ = 3419, 2960, 2930, 2934, 2875, 1684, 1630,

1473, 1435, 1283, 1242, 1114, 1063, 951, 751, 579 cm^{-1}. HRMS: calcd. for $C_{23}H_{29}NO_8$ 447.1893 $[M]^+$; found 447.1896.

1,1′-{2-[2-Oxo-2-(4-oxopiperidin-1-yl)ethyl]benzo(1,2-*d*:4,5-*d*′)bis([1,3]dioxole)-4,8-diyl}bis(butan-1-one) (20): Oxalyl chloride (1.4 mL, 0.34 mmol, 1.5 equiv.) was added dropwise to a solution of DMSO (33 μL, 0.46 mmol, 2.0 equiv.) in anhydrous DCM (10 mL) at –78 °C and the mixture stirred for 30 min. Compound **19** (102 mg, 0.28 mmol) dissolved in anhydrous DCM (3 mL) was added dropwise. After stirring for 30 min the reaction mixture was treated with NEt_3 (158 μL, 1.1 mmol, 5 equiv.) and stirred for 30 min while warming up to room temperature. DCM was added and the organic layer was washed with 1 N HCl and brine, dried with $MgSO_4$, evaporated, and the resulting residue purified by flash silica gel column chromatography (DCM/MeOH, 100:1) to yield **20** (59 mg, 0.13 mmol, 58 %) as an orange solid, m.p. 128–129 °C. ^1H NMR (300 MHz, $CDCl_3$): δ = 6.74 (t, ^3J = 4.9 Hz, 1 H), 6.10 (s, 2 H), 3.94 (t, ^3J = 6.3 Hz, 2 H), 3.81 (t, ^3J = 6.1 Hz, 2 H), 3.20 (d, ^3J = 4.9 Hz, 2 H), 2.88 (t, ^3J = 7.2 Hz, 4 H), 2.60–2.48 (m, 4 H), 1.70 (sext, ^3J = 7.3 Hz, 5 H), 0.96 (t, ^3J = 7.4 Hz, 7 H) ppm. ^{13}C NMR (75 MHz, $CDCl_3$): δ = 206.1, 196.2, 165.8, 141.0, 140.6, 111.1, 110.1, 102.5, 45.6, 44.4, 41.0, 40.9, 40.6, 38.6, 17.1, 13.7 ppm. IR (ATR): $\tilde{\nu}$ = 3623, 3421, 3188, 2960, 2930, 2874, 2754, 2601, 2547, 2292, 1706, 1681, 1468, 1435, 1416, 1399, 1367, 1347,1276,1242,1218,1126,1081,1038,986,960,931,737,663,620cm^{-1}. HRMS: calcd. for $C_{23}H_{27}NO_8$ 445.1737 $[M]^+$; found 445.1732.

8,8‴′-Dimethyl-6*H*,6‴′*H*-pentaspiro[[1,3]dioxolo[4,5-*g*]chromene-2,1′-cyclohexane-4′,2″-[1,3]dioxane-5″,5‴-[1,3]dioxane-2‴,1‴′-cyclohexane-4‴′,2‴′-[1,3]dioxolo[4,5-*g*]chromene]-6,6‴′-dione (22): NaH (9 mg, 0.22 mmol, 1.3 equiv.) and TMSCl (28 μL, 0.22 mmol, 1.3 equiv.) was added to a suspension of **5** (48 mg, 0.17 mmol) in anhydrous Et_2O (8 mL) at 0 °C. After stirring for 1 h, compound **21** (36 mg, 0.17 mmol, 1.0 equiv.) and 1 drop of TMSOTf were added and the suspension was stirred for 24 h at room temperature. The solvent was evaporated and the residue was purified by flash silica gel column chromatography (DCM/MeOH, 100:1) to yield **22** (47 mg, 0.07 mmol, 83 %) as a white solid, m.p. >220 °C (decomp.). ^1H NMR (300 MHz, [D_6]DMSO): δ = 7.22 (s, 2 H), 7.02 (s, 2 H), 6.20 (s, 2 H), 3.80–3.64 (m, 8 H), 2.34 (s, 6 H), 1.74–1.56 (m, 8 H), 1.51–1.28 (m, 8 H) ppm. ^{13}C NMR (75 MHz, [D_6]DMSO): δ = 160.4, 153.9, 150.3, 150.0, 144.2, 120.2, 113.4, 111.2, 103.1, 98.0, 96.5, 62.9, 62.1, 39.5, 32.2, 31.0, 28.6, 27.1, 18.8 ppm. IR (ATR): $\tilde{\nu}$ = 3057, 2962, 2925, 2858, 2800, 2364, 1621, 1584, 1493, 1441, 1398, 1377, 1342, 1270, 1223, 1207, 1159, 1139, 1088, 1043, 993, 970, 944, 909, 865, 807, 774, 735, 705, 690 cm^{-1}. HRMS: calcd. for $C_{37}H_{36}O_{12}$ 672.2207 $[M]^+$; found 672.2211.

2,2′-[(7,11,18,21-Tetraoxa-3,15-diazatrispiro[5.2.2.5^{12}.2^9.2^6]henicosane-3,15-diyl)bis(2-oxoethane-2,1-diyl)]bis(8-methyl-6*H*-[1,3]dioxolo[4,5-*g*]chromen-6-one) (23): NaH (13 mg, 320.39 μmol, 1.1 equiv.) and TMSCl (41 μL, 320.39 μmol, 1.1 equiv.) was added to a suspension of **8** (100 mg, 291.26 μmol) in anhydrous Et_2O (40 mL) at 0 °C. After stirring for 1 h, compound **21** (63 mg, 291.26 μmol, 1.0 equiv.) and 1 drop of TMSOTf were added and the suspension was stirred for 24 h at room temperature. The solvent was evaporated and the residue purified by flash silica gel column chromatography (DCM/MeOH, 100:1) to yield **23** (45 mg, 57.19 μmol, 39 %) as a white, vitreous solid. ^1H NMR (300 MHz, $CDCl_3$): δ = 6.91 (s, 2 H), 6.77 (s, 2 H), 6.71 (t, ^3J = 4.7 Hz, 2 H), 6.13 (s, 2 H), 3.86–3.76 (m, 4 H), 3.76–3.58 (m, 8 H), 3.53–3.36 (m, 4 H), 3.04 (d, ^3J = 4.7 Hz, 4 H), 2.34 (s, 6 H), 1.96–1.74 (m, 8 H) ppm. ^{13}C NMR (75 MHz, $CDCl_3$): δ = 165.4, 161.1, 152.3, 150.6, 150.5, 144.6, 113.8, 112.2, 110.9, 102.1, 98.3, 96.8, 63.4, 63.3, 38.5, 38.4, 33.8, 33.6, 33.2, 31.0, 30.9, 19.0 ppm. IR (ATR): $\tilde{\nu}$ = 3484, 3469, 2955, 2932, 2867, 2747, 2659, 1729, 1637, 1582, 1492, 1448, 1384, 1345, 1263, 1221, 1203, 1141, 1090, 1045, 962, 940, 920, 888, 863, 806, 744, 729, 711, 650 cm^{-1}. HRMS: calcd. for $C_{41}H_{42}N_2O_{14}$ 786.2636 $[M]^+$; found 786.2648.

(1,5-Dithiaspiro[5.5]undecane-3,3-diyl)dimethylenebis(oxytrimethylsilane) (25): NEt_3 (586 μL, 4.23 mmol, 5.0 equiv.) and TMSCl (536 μL, 4.23 mmol, 5.0 equiv.) were added to a suspension of **24** (210 mg, 0.85 mmol) in anhydrous toluene (30 mL). The mixture was stirred overnight at room temperature. The precipitate was filtered through Celite®, washed with petroleum ether (PE) and the solvent evaporated. The residue was treated with PE and filtered through Celite® once again. Removing of the solvent yielded **25** (333 mg, 0.85 mmol, 100 %) as a white solid. ^1H NMR (300 MHz, C_6D_6): δ = 3.72 (s, 4 H), 2.67 (s, 4 H), 2.06–1.89 (m, 4 H), 1.63–1.47 (m, 4 H), 1.32–1.19 (m, 2 H), 0.12 (s, 18 H) ppm. ^{13}C NMR (75 MHz, C_6D_6): δ = 64.0, 52.3, 38.9, 37.1, 29.9, 26.5, 23.1, 0.0 ppm, m.p. 70–72 °C. IR (ATR): $\tilde{\nu}$ = 2956, 2935, 2925, 2911, 2901, 2861, 2851, 1463, 1440, 1408, 1322, 1250, 1128, 1111, 1065, 1011, 876, 862, 833, 754, 746, 733, 687 cm^{-1}. HRMS: calcd. for $C_{17}H_{36}O_2S_2Si_2$: 392.1695 $[M]^+$; found 392.1689.

8‴″-Methyl-6‴″*H*-tetraspiro[cyclohexane-1,2′-[1,3]dithiane-5′,5″-[1,3]dioxane-2″,1‴-cyclohexane-4‴,2‴″-[1,3]dioxolo[4,5-*g*]chromen]-6‴″-one (26): NaH (9 mg, 0.22 mmol, 1.2 equiv.) and TMSCl (28 μL, 0.22 mmol, 1.2 equiv.) were added to a solution of **5** (53 mg, 0.18 mmol) in anhydrous Et_2O (30 mL) and DCM (5 mL) at 0 °C. After stirring for 1 h, **24** (50 mg, 0.20 mmol, 1.1 equiv.) and 1 drop of TMSOTf were added and the suspension was stirred at room temperature until complete conversion of **5**, monitored by TLC. The solvent was evaporated and the residue purified by flash silica gel column chromatography (DCM) to yield **26** (70 mg, 0.14 mmol, 74 %) as a white solid, m.p. >230 °C (decomp.). ^1H NMR (300 MHz, $CDCl_3$): δ = 6.89 (s, 1 H), 6.76 (s, 1 H), 6.14 (s, 1 H), 3.98–3.78 (m, 4 H), 2.74 (s, 4 H), 2.36 (s, 3 H), 2.15–2.02 (m, 8 H), 2.02–1.88 (m, 4 H), 1.72–1.55 (m, 4 H), 1.55–1.38 (m, 2 H) ppm. ^{13}C NMR (75 MHz, $CDCl_3$): δ = 161.4, 152.5, 150.7, 150.4, 144.7, 120.2, 113.4, 111.8, 102.0, 98.3, 97.1, 66.6, 66.5, 51.7, 37.6, 37.5, 31.2, 31.0, 29.1, 28.6, 25.8, 22.2, 19.1 ppm. IR (ATR): $\tilde{\nu}$ = 3525, 3505, 3485, 3415, 2931, 1723, 1624, 1580, 1499, 1449, 1401, 1376, 1344, 1301, 1272, 1235, 1220, 1204, 1139, 1123, 1109, 1085, 996, 954, 942, 921, 907, 850, 834, 768 cm^{-1}. HRMS: calcd. for $C_{27}H_{33}O_6S_2$ 517.1713 $[M + H]^+$; found 517.1703.

8-Methyl-2-[2-oxo-2-(7,21-dioxa-11,18-dithia-3-azatrispiro[5.2.2.5^{12}.29.26]henicosan-3-yl)ethyl]-6*H*-[1,3]dioxolo[4,5-*g*]chromen-6-one (27): NaH (13 mg, 0.32 mmol, 1.2 equiv.) and TMSCl (41 μL, 0.32 mmol, 1.2 equiv.) was added to a solution of **8** (92 mg, 0.27 mmol) in anhydrous Et_2O (20 mL) and DCM (2 mL) at 0 °C. After stirring for 1 h, **24** (70 mg, 0.28 mmol, 1.1 equiv.) and 1 drop of TMSOTf were added and the suspension was stirred at room temperature until complete conversion of **8**, monitored by TLC. The solvent was evaporated and the residue purified by flash silica gel column chromatography (DCM) to yield **27** (85 mg, 0.15 mmol, 55 %) as a white solid, m.p. >230 °C (decomp.). ^1H NMR (300 MHz, $CDCl_3$): δ = 6.93 (s, 1 H), 6.80 (s, 1 H), 6.73 (t, ^3J = 5.0 Hz, 1 H), 6.15 (s, 1 H), 3.94–3.78 (m, 4 H), 3.67 (t, ^3J = 5.4 Hz, 2 H), 3.52–3.40 (m, 2 H), 3.05 (d, ^3J = 5.1 Hz, 2 H), 2.77 (s, 2 H), 2.66 (s, 2 H), 2.35 (s, 3 H), 1.99–1.76 (m, 8 H), 1.68–1.54 (m, 4 H), 1.51–1.38 (m, 2 H) ppm. ^{13}C NMR (75 MHz, $CDCl_3$): δ = 165.4, 161.1, 152.4, 150.6, 150.5, 144.6, 113.8, 112.2, 110.9, 102.1, 98.4, 96.7, 66.3, 66.2, 51.6, 42.5, 38.5, 38.4, 37.5, 37.5, 33.7, 30.9, 30.9, 29.1, 25.7, 22.2, 19.1 ppm. IR (ATR): $\tilde{\nu}$ = 3518, 3484, 2930, 2855, 2777, 2751, 1726, 1635, 1583, 1493, 1449, 1405, 1386, 1345, 1298, 1264, 1220, 1204, 1141, 1108, 1081, 1035, 1012, 954, 918, 890, 862, 806, 778, 745 cm^{-1}. HRMS: calcd. for $C_{29}H_{35}NO_7S_2$ 573.1855 $[M]^+$; found 573.1851.

Benzyl {4,8-Dibutanoyltetraspiro[benzo(1,2-*d*:4,5-*d*′)bis[1,3]dioxole-2,1′-cyclohexane-4′,2″-[1,3]dioxane-5″,5‴-[1,3]dithiane-2‴,1⁗-cyclohexan]-6-yl}acetate (28): A drop of TMSOTf was added to a solution of **17** (20 mg, 37.27 μmol) and **25** (22 mg, 55.91 μmol, 1.5 equiv.) in anhydrous DCM (5 mL) and the reaction mixture was stirred overnight at room temperature. After evaporation of the solvent the residue was purified by flash silica gel column chromatography (DCM → DCM/MeOH, 100:1) to yield **28** (22 mg, 28.68 μmol, 78 %) as an orange solid, m.p. 161–163 °C. ^{1}H NMR (300 MHz, $CDCl_3$): δ = 7.45–7.30 (m, 5 H), 6.65 (t, ^3J = 5.0 Hz, 1 H), 5.19 (s, 2 H), 3.95–3.79 (m, 4 H), 3.11 (d, ^3J = 5.1 Hz, 2 H), 2.83 (t, ^3J = 7.2 Hz, 4 H), 2.77–2.68 (m, 4 H), 2.15–2.03 (m, 8 H), 2.03–1.92 (m, 4 H), 1.76–1.53 (m, 8 H), 1.53–1.37 (m, 2 H), 0.96 (t, ^3J = 7.3 Hz, 6 H) ppm. ^{13}C NMR (75 MHz, $CDCl_3$): δ = 196.4, 168.5, 151.8, 141.4, 128.6, 128.2, 110.9, 109.6, 99.6, 66.9, 66.5, 45.6, 41.1, 37.6, 32.2, 31.9 31.0, 30.9, 29.1, 22.2, 17.2, 13.8 ppm. IR (ATR): $\tilde{\nu}$ = 2960, 2933, 2870, 1739, 1687, 1465, 1442, 1398, 1377, 1299, 1281, 1271, 1246, 1188, 1122, 1110, 1038, 1005, 982, 958, 919, 903, 736, 696 cm^{-1}. HRMS: calcd. for $C_{41}H_{51}O_{10}S_2$ 767.2924 [M + H]$^+$; found 767.2925.

1,1′-{2-[2-Oxo-2-(7,21-dioxa-11,18-dithia-3-azatrispiro-[5.2.2.5^{12}.2^9.2^6]henicosan-3-yl)ethyl]benzo(1,2-*d*:4,5-*d*′)-bis([1,3]dioxole)-4,8-diyl}bis(butan-1-one) (29): A drop of TMSOTf was added to a solution of **20** (27 mg, 60.61 μmol) and **25** (36 mg, 90.92 μmol, 1.5 equiv.) in anhydrous DCM (10 mL) and the reaction mixture was stirred overnight at room temperature. After evaporation of the solvent the residue was purified by flash silica gel column chromatography (DCM → DCM/MeOH, 50:1) to yield **29** (38 mg, 56.23 μmol, 93 %) as an orange solid, m.p. 94–96 °C. ^{1}H NMR (300 MHz, $CDCl_3$): δ = 6.74 (t, ^3J = 4.3 Hz, 1 H), 6.10 (s, 2 H), 3.86 (br. s, 4 H), 3.72–3.61 (m, 2 H), 3.53–3.44 (m, 2 H), 3.16–3.06 (m, 2 H), 2.88 (t, ^3J = 7.2 Hz, 4 H), 2.79–2.61 (m, 4 H), 2.02–1.80 (m, 8 H), 1.76–1.56 (m, 8 H), 1.50–1.37 (m, 2 H), 0.97 (t, ^3J = 7.4 Hz, 6 H) ppm. ^{13}C NMR (75 MHz, $CDCl_3$): δ = 196.3, 165.2, 140.9, 140.6, 111.3, 110.0, 102.5, 96.7, 66.2, 51.6, 45.6, 42.6, 38.5, 38.4, 37.5, 33.5, 31.2, 30.9, 29.1, 25.7, 22.2, 17.1, 13.7 ppm. IR (ATR): $\tilde{\nu}$ = 2960, 2931, 2873, 2856, 1684, 1642, 1601, 1474, 1434, 1409, 1363, 1348, 1282, 1241, 1224, 1205, 1188, 1107, 1061, 1039, 1013, 951, 942, 934, 891, 864, 800, 732, 701, 597 cm^{-1}. HRMS: calcd. for $C_{34}H_{45}NO_9S_2$ 675.2536 [M]$^+$; found 675.2535.

5″,5″-Bis(hydroxymethyl)-8-methyl-6*H*-dispiro[[1,3]dioxolo-[4,5-*g*]chromene-2,1′-cyclohexane-4′,2″-[1,3]dithian]-6-one (31): A solution of **5** (249 mg, 869.77 μmol), **30** (380 mg, 956.75 μmol, 1.10 equiv.), and iodine (29 mg, 113.07 μmol, 0.13 equiv.) in DCM (20 mL) was stirred at room temperature until complete conversion of **5**, monitored by TLC. HF (48 %, 63 μL, 1.74 mmol, 2.00 equiv.) was added and the mixture stirred for a further 2 h. The organic layer was washed with aq. $NaHCO_3$ and aq. $Na_2S_2O_3$ (20 %), dried with $MgSO_4$, and the solvents evaporated. The residue was purified by flash silica gel column chromatography (DCM/MeOH, 100:1) to yield **31** (330 mg, 755.95 μmol, 87 %) as a white solid, m.p. >205 °C (decomp.). ^{1}H NMR (300 MHz, [D_6]-acetone): δ = 7.13 (s, 1 H), 6.83 (s, 1 H), 6.13 (s, 1 H), 3.89 (s, 4 H), 2.93–2.88 (m, 4 H), 2.41 (s, 3 H), 2.35–2.22 (m, 4 H), 2.21–2.10 (m, 4 H) ppm. ^{13}C NMR (75 MHz, $CDCl_3$): δ = 163.3, 154.9, 151.8, 151.0, 145.7, 120.8, 114.4, 111.8, 103.0, 98.8, 65.0, 64.9, 49.7, 44.6, 36.4, 35.2, 31.9, 30.1, 19.5 ppm. IR (ATR): $\tilde{\nu}$ = 3710, 2923, 2650, 2585, 2370, 2355, 1715, 1696, 1624, 1583, 1493, 1450, 1401, 1365, 1345, 1304, 1270, 1256, 1208, 1142, 1109, 1086, 1067, 968, 923, 838, 811, 745, 727 cm^{-1}. HRMS: calcd. for $C_{21}H_{25}O_6S_2$ 437.1093 [M + H]$^+$; found 437.1064.

8-Methyl-5″,5″-bis{[(trimethylsilyl)oxy]methyl}-6*H*-dispiro[[1,3]dioxolo[4,5-*g*]chromene-2,1′-cyclohexane-4′,2″-[1,3]-dithian]-6-one (32): Anhydrous NEt_3 (635 μL, 4.58 mmol, 10.0 equiv.) and TMSCl (582 μL, 4.58 mmol, 10.0 equiv.) were added to a suspension of **31** (200 mg, 0.46 mmol) in anhydrous toluene (10 mL). The reaction mixture was stirred overnight at room temperature, filtered through Celite®, washed with PE, and the solvent evaporated. The residue was suspended in PE and filtered through Celite® once more. Evaporation of the solvent yielded **32** (266 g, 0.46 mmol, quant.) as a white solid, m.p. 142–144 °C. ^{1}H NMR (300 MHz, $CDCl_3$): δ = 6.55 (s, 1 H), 6.40 (s, 1 H), 5.84 (d, ^4J = 1.1 Hz, 1 H), 3.71 (s, 4 H), 2.63 (s, 4 H), 2.25–2.14 (m, 4 H), 2.05–1.94 (m, 4 H), 1.50 (d, ^4J = 1.1 Hz, 3 H), 0.16–0.10 (m, 19 H) ppm. ^{13}C NMR (75 MHz, $CDCl_3$): δ = 160.5, 151.5, 151.5, 151.0, 144.8, 120.0, 114.0, 113.1, 102.7, 98.8, 63.9, 49.7, 44.5, 36.8, 35.3, 31.9, 30.2, 18.7, –0.08 ppm. IR (ATR): $\tilde{\nu}$ = 3055, 2956, 2930, 2914, 2858, 1726, 1633, 1620, 1580, 1489, 1439, 1360, 1344, 1225, 1208, 1158, 1135, 1116, 1091, 1065, 1042, 967, 947, 921, 906, 872, 838, 809, 748, 690 cm^{-1}. HRMS: calcd. for $C_{27}H_{40}O_6S_2Si_2$ 580.1805 [M]$^+$; found 580.1812.

Benzyl 2-{4,8-Dibutyryl-8⁗′-methyl-6⁗′-oxo-6⁗′*H*-pentaspiro[benzo(1,2-*d*:4,5-*d*′)bis([1,3]dioxole)-2,1′-cyclohexane-4′,2″-[1,3]dioxane-5″,5‴-[1,3]dithiane-2⁗,1⁗′-cyclohexane-4⁗′,2⁗′-[1,3]dioxolo[4,5-*g*]chromen]-6-yl}acetate (33): A drop of TMSOTf was added to a solution of **17** (20 mg, 37.27 μmol) and **32** (24 mg, 41.00 μmol, 1.1 equiv.) in anhydrous DCM (5 mL) and the reaction mixture was stirred overnight at room temperature. After evaporation of the solvent the residue was purified by flash silica gel column chromatography (DCM → DCM/MeOH, 50:1) to yield **33** (23 mg, 24.08 μmol, 64 %) as an orange solid, m.p. 115 °C. ^{1}H NMR (300 MHz, $CDCl_3$): δ = 7.42–7.29 (m, 5 H), 6.90 (s, 1 H), 6.77 (s, 1 H), 6.66 (t, ^3J = 4.9 Hz, 1 H), 6.15 (s, 1 H), 5.19 (s, 2 H), 3.90 (s, 4 H), 3.11 (d, ^3J = 4.9 Hz, 2 H), 2.90–2.72 (m, 8 H), 2.36 (s, 3 H), 2.32–2.21 (m, 4 H), 2.21–1.97 (m, 12 H), 1.78–1.59 (m, 4 H), 0.96 (t, ^3J = 7.3 Hz, 6 H) ppm. ^{13}C NMR (125 MHz, $CDCl_3$): δ = 196.4, 167.5, 161.4, 152.5, 150.6, 150.4, 144.5, 140.8, 139.9, 135.2, 128.6, 128.4, 128.2, 120.4, 119.6, 113.5, 111.9, 110.1, 109.6, 102.0, 98.3, 97.2, 66.9, 66.4, 49.3, 45.6, 40.0, 36.9, 34.2, 31.3, 31.2, 31.0, 29.0, 19.1, 17.2, 13.8 ppm. IR (ATR): $\tilde{\nu}$ = 2961, 2931, 2872, 2851, 1725, 1687, 1637, 1627, 1585, 1495, 1440, 1403, 1377, 1348, 1283, 1273, 1259, 1225, 1207, 1140, 1107, 1067, 1043, 1012, 969, 922, 905, 863, 802, 744 cm^{-1}. HRMS: calcd. for $C_{51}H_{54}O_{14}S_2$ 955.3033 [M]$^+$; found 955.3015.

1,1′-[2-(2-{8⁗′-Methyl-6⁗′-oxo-6⁗′*H*-tetraspiro[piperidine-4,2′-[1,3]dioxane-5′,5″-[1,3]dithiane-2″,1‴-cyclohexane-4‴,2⁗′-[1,3]dioxolo[4,5-*g*]chromen]-1-yl}-2-oxoethyl)benzo(1,2-*d*:4,5-*d*′)bis([1,3]dioxole)-4,8-diyl]bis(butan-1-one) (34): A drop of TMSOTf was added to a solution of **32** (40 mg, 68.86 μmol) and **20** (34 mg, 75.74 μmol, 1.1 equiv.) in anhydrous DCM (10 mL) and the reaction mixture was stirred overnight at room temperature. After evaporation of the solvent the residue was purified by flash silica gel column chromatography (DCM → DCM/MeOH, 50:1) to yield **34** (30 mg, 34.72 μmol, 50 %) as an orange solid, m.p. 113 °C. ^{1}H NMR (300 MHz, $CDCl_3$): δ = 6.89 (s, 1 H), 6.82–6.65 (m, 2 H), 6.25–6.02 (m, 3 H), 3.97–3.80 (m, 4 H), 3.72–3.62 (m, 2 H), 3.54–3.41 (m, 2 H), 3.11 (d, ^3J = 4.1 Hz, 2 H), 2.88 (t, ^3J = 7.2 Hz, 4 H), 2.84–2.65 (m, 4 H), 2.35 (s, 3 H), 2.30–2.19 (m, 4 H), 2.18–2.09 (m, 4 H), 1.94–1.81 (m, 4 H), 1.77–1.62 (m, 4 H), 0.97 (t, ^3J = 7.4 Hz, 6 H) ppm. ^{13}C NMR (75 MHz, $CDCl_3$): δ = 196.4, 165.3, 161.3, 152.4, 150.5, 150.4, 144.5, 141.0, 140.6, 119.6, 113.5, 111.9, 111.3, 110.0, 102.5, 102.0, 98.3, 96.9, 66.1, 49.2, 45.6, 42.6, 38.5, 38.4, 34.1, 33.6, 31.3, 31.2, 29.1, 19.1, 17.1, 13.7 ppm. IR (ATR): $\tilde{\nu}$ = 3423, 3364, 3064, 2961, 2933, 2874, 2251, 1718, 1686, 1639, 1584, 1495, 1474, 1451, 1436, 1403, 1368, 1347, 1282, 1273, 1259, 1242, 1224, 1141, 1108, 1067, 1045, 925, 906, 863, 812, 773, 731, 647, 596, 496 cm^{-1}. HRMS: calcd. for $C_{44}H_{49}NO_{13}S_2$ 863.2645 [M]$^+$; found 863.2668.

Acknowledgments

The financial support of this work by the Deutsche Forschungsgemeinschaft (DFG) (WE 1850/10-1 and KU 1162/12-1) is gratefully acknowledged.

Keywords: Fluorescence · Energy transfer · FRET · Chromophores · Spiro compounds

[1] a) M. D. Brenner, R. Zhou, T. Ha, *Biopolymers* **2011**, *95*, 332; b) D. M. Morris, G. J. Jensen, *Ann. Rev. Biochem.* **2008**, *77*, 583; c) A. L. Plant, K. Bhadriraju, T. A. Spurlin, J. T. Elliott, *Biochim. Biophys. Acta – Mol. Cell Res.* **2009**, *1793*, 893.

[2] C. Yang, X. Zhang, Y. Guo, F. Meng, F. Sachs, J. Guo, *Biochim. Biophys. Acta – Mol. Cell Res.* **2015**, *1853*, 1889.

[3] a) B. Liu, W. Chen, C. Zhu, *Ann. Rev. Phys. Chem.* **2014**, *66*, 427; b) B. Hochreiter, A. P. Garcia, J. A. Schmid, *Sensors* **2015**, *15*, 26281; c) C. Jurchenko, K. S. Salaita, *Mol. Cell. Biol.* **2015**, *35*, 2570; d) B. Kainz, E. A. Oprzeska-Zingrebe, J. L. Herrera, *Biotechnol. J.* **2014**, *9*, 51; e) D. Shrestha, A. Jenei, P. Nagy, G. Vereb, J. Szöllösi, *Int. J. Mol. Sci.* **2015**, *16*, 6718.

[4] a) B. W. Van Der Meer, *Rev. Mol. Biotechnol.* **2002**, *82*, 181; b) B. W. Van der Meer, *Forster Theory*, in: *FRET Förster Resonance Energy Transfer: From Theory to Applications* (Eds.: I. Medintz, N. Hildebrandt), Wiley-VCH, Weinheim, Germany, **2014**, p. 23–62.

[5] D. B. VanBeek, M. C. Zwier, J. M. Shorb, B. P. Krueger, *Biophys. J.* **2007**, *92*, 4168.

[6] H. Langhals, A. J. Esterbauer, A. Walter, E. Riedle, E. I. Pugliesi, *J. Am. Chem. Soc.* **2010**, *132*, 16777.

[7] a) P. Wessig, K. Möllnitz, C. Eiserbeck, *Chem. Eur. J.* **2007**, *13*, 4859; b) P. Wessig, K. Möllnitz, *J. Org. Chem.* **2008**, *73*, 4452; c) P. Müller, J. Nikolaus, S. Schiller, A. Herrmann, K. Möllnitz, S. Czapla, P. Wessig, *Angew. Chem. Int. Ed.* **2009**, *48*, 4433; *Angew. Chem.* **2009**, *121*, 4497; d) J. Nikolaus, S. Czapla, K. Möllnitz, C. T. Höfer, A. Herrmann, P. Wessig, P. Müller, *Biochim. Biophys. Acta (BBA) - Biomembranes* **2011**, 2781; e) P. Wessig, K. Möllnitz, *J. Org. Chem.* **2012**, *77*, 3907; f) C. Grimm, T. Meyer, S. Czapla, J. Nikolaus, H. A. Scheidt, A. Vogel, A. Herrmann, P. Wessig, D. Huster, P. Müller, *Chem. Eur. J.* **2013**, *19*, 2703; g) A. Techen, S. Czapla, K. Möllnitz, D. Budach, P. Wessig, M. U. Kumke, *Helv. Chim. Acta* **2013**, *96*, 2046; h) P. Wessig, M. Gerngroß, S. Pape, P. Bruhns, J. Weber, *RSC Adv.* **2014**, *4*, 31123; i) P. Wessig, D. Budach, A. Thünemann, *Chem. Eur. J.* **2015**, *21*, 10466; j) P. Wessig, R. Merkel, P. Müller, *Beilstein J. Org. Chem.* **2015**, *11*, 74.

[8] P. Wessig, M. Gerngroß, D. Freyse, P. Bruhns, M. Przezdziak, U. Schilde, A. Kelling, *J. Org. Chem.* **2016**, *81*, 1125.

[9] a) P. Wessig, R. Wawrzinek, K. Möllnitz, E. Feldbusch, U. Schilde, *Tetrahedron Lett.* **2011**, *52*, 6192; b) R. Wawrzinek, P. Wessig, K. Möllnitz, J. Nikolaus, R. Schwarzer, P. Müller, A. Herrmann, *Bioorg. Med. Chem. Lett.* **2012**, *22*, 5367; c) R. Wawrzinek, J. Ziomkowska, J. Heuveling, M. Mertens, A. Herrmann, E. Schneider, P. Wessig, *Chem. Eur. J.* **2013**, *19*, 17349; d) J. Heuveling, V. Frochaux, J. Ziomkowska, R. Wawrzinek, P. Wessig, A. Herrmann, E. Schneider, *Biochim. Biophys. Acta (BBA) - Biomembranes* **2014**, *1838*, 106; e) C. Meyners, R. Wawrzinek, A. Krämer, S. Hinz, P. Wessig, F.-J. Meyer-Almes, *Anal. Bioanal. Chem.* **2014**, 4889; f) R. Wawrzinek, P. Wessig, *Dyes Pigm.* **2015**, *123*, 39; g) D. Bader, D. T. Klier, C. Hettrich, F. F. Bier, P. Wessig, *Anal. Methods* **2016**, *8*, 1235.

[10] P. Wessig, N. Behrends, M. U. Kumke, U. Eisold, T. Meiling, C. Hille, *RSC Adv.* **2016**, *6*, 33510.

[11] T. Tsunoda, M. Suzuki, R. Noyori, *Tetrahedron Lett.* **1980**, *21*, 1357.

[12] K. Kumamoto, Y. Ichikawa, H. Kotsuki, *Synlett* **2005**, 2254.

[13] H. H. Hussain, G. Babic, T. Durst, J. S. Wright, M. Flueraru, A. Chichirau, L. L. Chepelev, *J. Org. Chem.* **2003**, *68*, 7023.

[14] X. Ariza, O. Pineda, J. Vilarrasa, G. W. Shipps Jr., Y. Ma, X. Dai, *Org. Lett.* **2001**, *3*, 1399.

[15] M. C. Murguia, S. E. Vaillard, R. J. Grau, *Synthesis* **2001**, 1093.

[16] H. J. Backer, A. F. Tamsma, *Rec. Trav. Chim.* **1938**, *57*, 1183.

[17] A. Muñoz-Losa, C. Curutchet, B. P. Krueger, L. R. Hartsell, B. Mennucci, *Biophys. J.* **2009**, *96*, 4779.

[18] P. Nalbach, I. Pugliesi, H. Langhals, M. Thorwart, *Phys. Rev. Lett.* **2012**, *108*, 1.

Received: April 19, 2016
Published Online: ■

FRET Rods

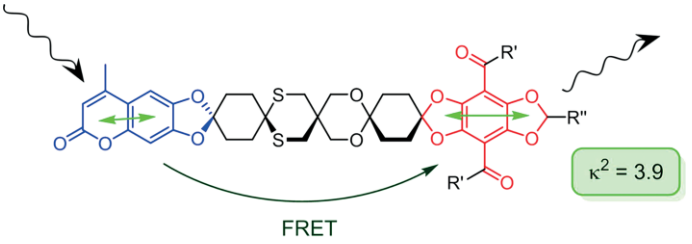

FRET pairs with a fixed relative orientation of chromophores have been synthesized by combining fluorophores with oligo-spirothioketal (OSTK) rods. Their photophysical properties have been investigated and are described herein.

DOI: 10.1002/ejoc.201600489